

# Assessing the bone-healing potential of bone marrow mesenchymal stem cells in jawbone osteoporosis in albino rats

Tasneem Soliman<sup>1,2,A–F</sup>, Zoba Ali<sup>1,A–F</sup>, Mohamed Zayed<sup>2,A,E,F</sup>, Dina Sabry<sup>3,4,C,E,F</sup>, Nermeen AbuBakr<sup>1,5,A–F</sup>

<sup>1</sup> Department of Oral Biology, Faculty of Dentistry, Cairo University, Egypt

<sup>2</sup> Department of Oral Biology, Faculty of Dentistry, Misr International University, Cairo, Egypt

<sup>3</sup> Department of Medical Biochemistry and Molecular Biology, Faculty of Medicine, Cairo University, Egypt

<sup>4</sup> Department of Medical Biochemistry and Molecular Biology, Faculty of Medicine, Badr University in Cairo, Badr, Egypt

<sup>5</sup> Stem Cells and Tissue Engineering Unit, Faculty of Dentistry, Cairo University, Egypt

A – research concept and design; B – collection and/or assembly of data; C – data analysis and interpretation;

D – writing the article; E – critical revision of the article; F – final approval of the article

Dental and Medical Problems, ISSN 1644-387X (print), ISSN 2300-9020 (online)

*Dent Med Probl.* 2022;59(1):75–83

## Address for correspondence

Nermeen AbuBakr

E-mail: nermeen.abubakr@dentistry.cu.edu.eg

## Funding sources

None declared

## Conflict of interest

None declared

## Acknowledgements

None declared

Received on February 10, 2021

Reviewed on June 15, 2021

Accepted on June 21, 2021

Published online on March 4, 2022

## Cite as

Soliman T, Ali Z, Zayed M, Sabry D, AbuBakr N. Assessing the bone-healing potential of bone marrow mesenchymal stem cells in jawbone osteoporosis in albino rats. *Dent Med Probl.* 2022;59(1):75–83. doi:10.17219/dmp/139200

## DOI

10.17219/dmp/139200

## Copyright

© 2022 by Wrocław Medical University

This is an article distributed under the terms of the

Creative Commons Attribution 3.0 Unported License (CC BY 3.0)

(<https://creativecommons.org/licenses/by/3.0/>).

## Abstract

**Background.** Osteoporosis is one of the most common yet difficult to treat diseases. It affects millions of people and costs the health care systems billions worldwide. All of the available kinds of pharmacological treatment have multiple side effects, which is why a need for safer treatment options has emerged.

**Objectives.** This study aimed to assess the bone-healing potential of bone marrow mesenchymal stem cells (BM-MSCs) in jawbone osteoporosis in Wistar albino rats.

**Material and methods.** Osteoporosis was induced with a daily intraperitoneal injection of 200 µg/100 g dexamethasone for 1 month. The rats were then randomly distributed into 2 groups: the osteoporotic group (left untreated); and the BM-MSCs group (received an intravenous injection of 50 million cultured BM-MSCs). Half of the rats from each group were sacrificed 2 weeks and the other half 6 weeks after the introduction of treatment. Bone regeneration was assessed by means of dual-energy X-ray absorptiometry (DEXA), real-time polymerase chain reaction (RT-PCR), as well as the histopathological and histomorphometric analyses.

**Results.** As for the 1<sup>st</sup> sacrifice time, there were no significant differences between the osteoporotic and BM-MSCs groups with regard to all parameters except for bone mineral density (BMD), which was significantly higher in the BM-MSCs group. Regarding the 2<sup>nd</sup> sacrifice time, the DEXA analysis showed a significant increase in BMD in the BM-MSCs group ( $p < 0.001$ ). The RT-PCR analysis showed a significant decrease in *RANKL* gene expression ( $p < 0.001$ ) and a significant increase in *OPG* gene expression ( $p < 0.001$ ) in the BM-MSCs group. In addition, the histopathological examination of the BM-MSCs group showed pronounced healing progress in the jawbone microarchitecture. The histomorphometric analysis also revealed that the bone area percentage significantly increased in the BM-MSCs group ( $p < 0.001$ ).

**Conclusions.** This study proved that BM-MSCs could be effective in the treatment of osteoporosis.

**Keywords:** mesenchymal stem cells, bone regeneration, osteoporosis, bone marrow

## Introduction

Osteoporosis is a “progressive skeletal systemic disease characterized by reduced bone mass and micro-architectural deterioration, with a subsequent rise in bone fragility and fracture susceptibility”.<sup>1</sup> It is the most common bone disease in humans, representing a major public health problem worldwide.<sup>2</sup>

Osteoporosis causes the loss of bone mineral density (BMD) throughout the body, including the maxillary and mandibular bones. This reduced jawbone density leads to the increased porosity and accelerated resorption of the alveolar bone. Since the alveolar processes provide the teeth with support, their reduced bone density can have negative consequences on tooth stability.<sup>3</sup>

Glucocorticoid-induced osteoporosis may happen in 30–50% of patients on glucocorticoid therapy. It is the main iatrogenic cause of secondary osteoporosis. Glucocorticoids increase the production of macrophage colony-stimulating factor (M-CSF) and receptor activator of nuclear factor kappa-beta ligand (RANKL), and decrease the production of osteoprotegerin (OPG), subsequently increasing the number and activity of osteoclasts.<sup>4</sup>

The pharmacological treatment of osteoporosis has been proven to have many side effects. Oral bisphosphonates, such as ibandronate, alendronate and risedronate, can cause upper gastrointestinal irritation and flu-like symptoms.<sup>5,6</sup> Intravenous amino-bisphosphonates, such as ibandronate and zoledronate, are potentially nephrotoxic, and can cause hypocalcemia and atrial fibrillation. They also pose an increased risk of heart failure, which is mostly due to the increased incidence of hyperlipidemia, hypertension and peripheral artery disease among these patients.<sup>5–7</sup> Raloxifene can cause venous thromboembolism, whereas teriparatide has triggered concerns about osteosarcoma in animal studies.<sup>5</sup>

Mesenchymal stem cells (MSCs) obtained from bone marrow (BM) can be separated easily, have the ability to self-renew, proliferate and differentiate into multilineages, retain the ‘homing’ feature, and are characterized by long storage without major loss of potency, thus making them the first option in repairing bone and treating related diseases.<sup>8,9</sup>

Bone regeneration is a complex process involving the interrelation between adipogenic and osteogenic progenitor cells, which are both derived from BM.<sup>10</sup> It has been confirmed that BM-MSCs can be differentiated into osteoblasts and secrete many osteogenic factors after being cultured in vitro. They have also been proven to have great potential in bone and soft tissue repair in vivo. Moreover, they can migrate to the site of injury, creating an appropriate microenvironment for tissue repair.<sup>11,12</sup>

In this context, this study aimed to assess the bone healing potential of BM-MSCs in glucocorticoid-induced jawbone osteoporosis by evaluating BMD as a primary outcome in addition to the gene expression of *RANKL* and *OPG*, histopathological alterations, and the histomorphometric analysis of the jawbones as secondary outcomes.

## Material and methods

This experiment was conducted at the animal house at the Faculty of Medicine of Cairo University, Egypt, after obtaining the approval of the Institutional Animal Care and Use Committee (IACUC) (CU-III-F-73-17).

### Isolation and culture of BM-MSCs

Bone marrow was flushed out of the tibias of male albino rats with an approximate weight of 100–120 g and age of 6 weeks by using phosphate buffered saline (PBS) (Invitrogen, Grand Island, USA) and centrifuged at 1,000 rpm for 5 min. A total of 35 mL of the flushed BM cells was layered over 15 mL Ficoll-Paque™ (Invitrogen) and centrifuged at  $400 \times g$  for 35 min. The upper layer was discarded, leaving a mononuclear cell (MNC) layer at the interphase. This MNC layer was collected, washed twice in PBS, and centrifuged at  $200 \times g$  for 10 min at 10°C. The isolated BM-MSCs were cultured and propagated in 25-milliliter culture flasks with RPMI-1640 (Merck, Darmstadt, Germany) supplemented with 10% fetal bovine serum (FBS) (Thermo Fisher Scientific, Waltham, USA), 0.5% penicillin (Thermo Fisher Scientific) and streptomycin (Thermo Fisher Scientific). It was subsequently incubated at 5% CO<sub>2</sub> and 37°C until reaching 80–90% confluence within 14 days of culture.<sup>13</sup>

### Identification of BM-MSCs in the culture

Bone marrow MSCs were characterized in accordance with the International Society for Cellular Therapy guidelines<sup>14</sup> in terms of their morphology, adherence, fluorescence-activated cell sorting (FACS) by assessing positivity for CD90<sup>+</sup>, CD105<sup>+</sup> and CD73<sup>+</sup>, and negativity for CD14<sup>-</sup>, CD34<sup>-</sup> and CD45<sup>-</sup>, and their capability to differentiate into osteoblasts, adipocytes and chondroblasts. The differentiation of BM-MSCs into osteoblasts was performed using a StemPro™ osteogenesis differentiation kit (Life Technologies, Carlsbad, USA); the cells were stained with the Alizarin Red S stain (Sigma-Aldrich, St. Louis, USA). Adipocyte differentiation was achieved with a StemPro™ adipogenesis differentiation kit (Life Technologies), and the cells were subsequently stained with the Oil Red O stain (Sigma-Aldrich). Chondroblast differentiation was performed using a StemPro™ chondrogenesis differentiation kit (Life Technologies), after which the cells were stained with the Alcian Blue stain (Sigma-Aldrich).

### Sample size

The sample size was calculated using the G\*power software (<https://www.psychologie.hhu.de/arbeitsgruppen/allgemeine-psychologie-und-arbeitspsychologie/gpower>). In terms of the primary outcome (BMD) based on Uejima et al., the results revealed  $124.32 \pm 4.88$  mg/cm<sup>2</sup> for the control bones and  $139.35 \pm 4.63$  mg/cm<sup>2</sup> for the BM-MSCs-injected

bones<sup>15</sup>; it was found that 3 rats per group with a total sample size of 12 rats was the appropriate sample size for the study (2 groups per each duration of 2 and 6 weeks). The power was 80% and the  $\alpha$  error probability 0.05. The number was increased to 4 rats in each group to compensate for possible losses during the experiment for a total of 16 rats ( $4 \times 4$ ). The magnitude of the effect to be detected was estimated as mean and standard deviation ( $M \pm SD$ ) for the variable of interest, and was obtained from the scientific literature (Uejima et al.<sup>15</sup>).

## Experimental animals

A total of 16 healthy male Wistar albino rats (*Rattus norvegicus*) with an approximate weight of 150–200 g and age of 3–4 months were obtained from the animal house at the Faculty of Medicine of Cairo University. The animals were housed in a controlled, sterile environment (temperature  $23 \pm 5^\circ\text{C}$  and 12-hour dark/light cycles). They had free access to a standard pellet diet and tap water ad libitum. They were maintained individually in stainless steel cages and kept under good ventilation. Each individual rat was considered an experimental unit within this study.

## Study design

The animals were randomly divided using the Random Sequence Generator program (<https://www.random.org/>). Each animal was assigned a temporary random number. The rats were divided into 2 groups of 8 rats each (4 for each sacrifice date) as follows:

- the osteoporotic group consisted of 8 glucocorticoid-induced osteoporotic rats; these rats received no treatment and served as a positive control group;
- the BM-MSCs group consisted of 8 glucocorticoid-induced osteoporotic rats; these rats received a single intravenous injection of 50 million cultured BM-MSCs in PBS through the tail vein.<sup>16</sup>

## Experimental procedure

The experiment was held at the animal house at the Faculty of Medicine of Cairo University. Four investigators were involved for each animal; the 1<sup>st</sup> investigator was the only one aware of group allocation. During the experimental procedure, the 2<sup>nd</sup> investigator was the only person to assess dosage administration for all animals. The 3<sup>rd</sup> investigator assessed the outcomes in a masked fashion, without knowing the groups. The statistician performed data analysis and was unaware of group allocation. All rats were intraperitoneally injected with 200  $\mu\text{g}/100\text{ g}$  dexamethasone (Amriya Pharmaceuticals, Alexandria, Egypt) once daily for 30 days to induce osteoporosis.<sup>17</sup> Bone mineral density was measured at the jawbone to confirm that the model was successfully established. Both the rats in the BM-MSCs group and the rats

in the untreated osteoporotic group were sacrificed 2 and 6 weeks after the introduction of treatment. The animals were sacrificed using an intraperitoneal overdose injection of an anesthetic mixture (ketamine/xylazine) (Sigma-Aldrich).<sup>18</sup> Each lower jaw was dissected and processed for the assessment of the experimental outcomes.

## Experimental outcomes

### Dual-energy X-ray absorptiometry (DEXA) (primary outcome)

The BMD of the mandibles was measured using dual-energy X-ray absorptiometry (DEXA). A Norland XR-46 DXA scanner (Norland Corp., Fort Atkinson, USA), equipped with the appropriate software for bone assessment, was utilized. The scan resolution was  $0.5 \times 0.5\text{ mm}$  and the scan speed was 60 mm/s. The analysis was carried out based on the image of the animal's jawbone on the screen, using a region of interest (ROI), which was defined to include the bone area below the first molar. The results were displayed automatically in  $\text{g}/\text{cm}^2$ .<sup>19</sup>

### Real-time polymerase chain reaction (RT-PCR) (secondary outcome)

Total RNA was extracted for further real-time polymerase chain reaction (RT-PCR) analysis. RNA was isolated with an RNeasy Micro Kit (Cat. No./ID: 74004; Qiagen, Hilden, Germany). A total of 20 ng of the isolated total RNA was used to develop cDNA by means of a high-capacity cDNA Reverse Transcription Kit (Cat. No: 4368814; Applied Biosystems, Foster City, USA). The PCR analysis was performed using a SYBR<sup>®</sup> Green Master Mix kit (Cat. No: 4344463; Applied Biosystems) with the StepOnePlus<sup>™</sup> Real-Time PCR System (Applied Biosystems), according to standard protocols. Briefly, the RT-PCR thermal profile was programmed as follows: 10 min at  $45^\circ\text{C}$  for reverse transcription; 2 min at  $98^\circ\text{C}$  for the inactivation of reverse transcriptase (RT); and initial denaturation with 40 cycles of 10 s at  $98^\circ\text{C}$ , 10 s at  $55^\circ\text{C}$  and 30 s at  $72^\circ\text{C}$  for the amplification step. The relative quantity (RQ) values for each target gene were measured according to the calculation of  $\Delta\Delta\text{Ct}$ . The calculation of the RQ values for the studied genes was performed by  $2^{-\Delta\Delta\text{Ct}}$  normalization to the house-keeping gene *GADPH*. The primers for *RANKL*, *OPG* and *GADPH* are shown in Table 1.

Table 1. Primer sequences specific for each gene

Gene symbol	Primer sequences from 5' to 3'
<i>RANKL</i>	F: ACC AGC ATC AAA ATC CCA AG R: TTT GAA AGC CCC AAA GTA CG
<i>OPG</i>	F: GTT CTT GCA CAG CTT CAC CA R: AAA CAG CCC AGT GAC CAT TC
<i>GAPDH</i>	F: GACGGCCGCATCTTCTTGA R: CACACCGACCTTCAACATTT

### Histopathological examination (secondary outcome)

The specimens were decalcified for 4 weeks, dehydrated in ascending grades of alcohol, cleared in xylol, and embedded in paraffin blocks. Serial sections of a thickness of 5–6  $\mu\text{m}$  were cut, mounted on glass slides, and stained with hematoxylin and eosin (H&E) for a routine histopathological examination.

### Histomorphometric analysis (secondary outcome)

The area percentage of bone in the region below the first molar for each specimen was measured. The data was obtained using a Leica Qwin 500 image analyzer computer system (Wetzlar, Germany). The area and area percentage of bone trabeculae were measured with an objective lens magnification of  $\times 20$  (a total magnification of  $\times 200$ ). Five fields were measured for each specimen. The bone area percentage was calculated in relation to a standard measuring frame having an area of 118,476.6  $\mu\text{m}^2$ .

### Statistical analysis

The data was coded and processed using the IBM SPSS Statistics for Windows software, v. 24.0 (IBM Corp., Armonk, USA). The data was presented as  $M \pm SD$ . The Kolmogorov–Smirnov test showed that the data was normally distributed; thus, comparisons between the 2 groups were performed using the independent  $t$  test. A  $p$ -value  $\leq 0.05$  was considered statistically significant.

## Results

### Morphological characterization of BM-MSCs

The morphology of BM-MSCs was observed under an inverted microscope (Invitrogen, Waltham, USA). Bone marrow MSCs were expanded successfully and adhered to culture flasks, showing a heterogeneous population, displaying fibroblast-like morphology and forming a confluent monolayer at 14 days of culture (Fig. 1(I)A). Bone marrow MSCs were differentiated into osteoblasts, stained with Alizarin Red S (Fig. 1(I)B), adipocytes, stained with Oil Red O (Fig. 1(I)C), and chondroblasts, stained with Alcian Blue (Fig. 1(I)D).

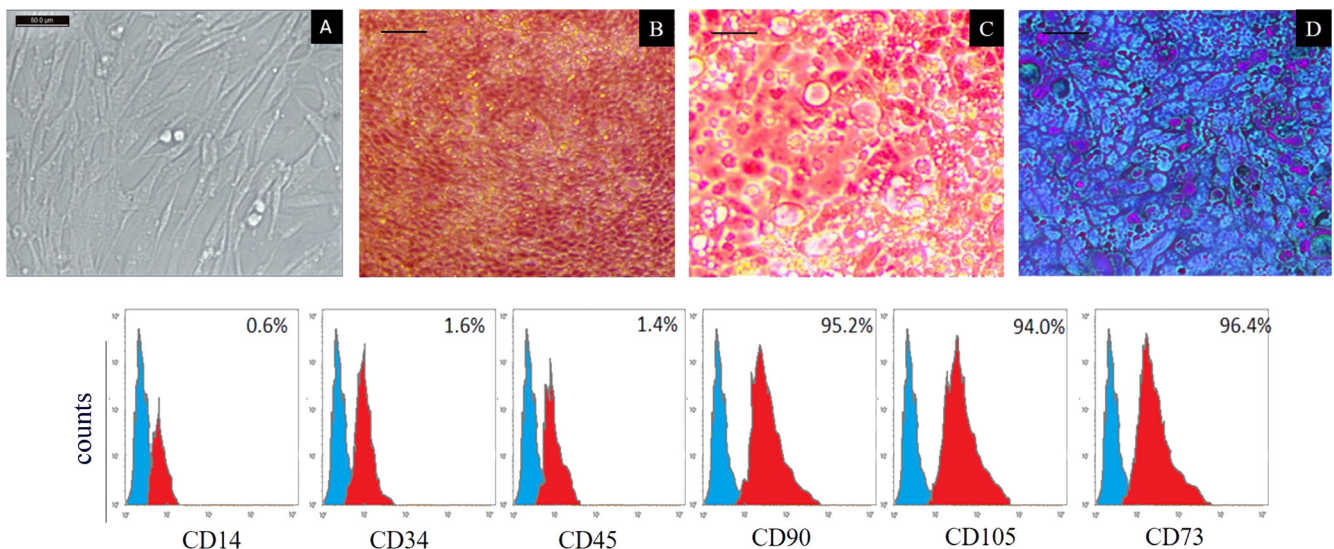
### Phenotypic characterization of BM-MSCs

The phenotypic FACS analysis revealed that BM-MSCs were positive for CD90<sup>+</sup> (95.2%), CD105<sup>+</sup> (94.0%) and CD73<sup>+</sup> (96.4%), and negative for CD14<sup>−</sup> (0.6%), CD34<sup>−</sup> (1.6%) and CD45<sup>−</sup> (1.4%) (Fig. 1(II)).

### DEXA results

A significant increase in BMD was observed in the BM-MSCs group as compared to the osteoporotic group at the 1<sup>st</sup> and 2<sup>nd</sup> sacrifice times ( $p < 0.001$ ) (Table 2).

#### I – BM-MSCs in culture



#### II – FACS analysis of BM-MSCs

**Fig. 1.** (I) Bone marrow mesenchymal stem cells (BM-MSCs) in culture: A – plastic adherence and spindle-shaped morphology at 14 days of culture (scale bar: 50  $\mu\text{m}$ ); B – BM-MSCs differentiated into osteoblasts, stained with Alizarin Red S (scale bar: 100  $\mu\text{m}$ ); C – BM-MSCs differentiated into adipocytes, stained with Oil Red O (scale bar: 100  $\mu\text{m}$ ); D – BM-MSCs differentiated into chondroblasts, stained with Alcian Blue (scale bar: 100  $\mu\text{m}$ ); (II) fluorescence-activated cell sorting (FACS) analysis of BM-MSCs: positive for CD90<sup>+</sup> (95.2%), CD105<sup>+</sup> (94.0%) and CD73<sup>+</sup> (96.4%), and negative for CD14<sup>−</sup> (0.6%), CD34<sup>−</sup> (1.6%) and CD45<sup>−</sup> (1.4%)



**Table 2.** Dual-energy X-ray absorptiometry (DEXA), real-time polymerase chain reaction (RT-PCR) and histomorphometric results

Analysis	1 <sup>st</sup> sacrifice time			2 <sup>nd</sup> sacrifice time		
	osteoporotic group	BM-MSCs group	<i>p</i> -value	osteoporotic group	BM-MSCs group	<i>p</i> -value
DEXA (BMD [g/cm <sup>2</sup> ])	0.05 ±0.01	0.09 ±0.01	<0.001*	0.02 ±0.01	0.10 ±0.02	<0.001*
<i>RANKL</i> gene expression [AU]	1.64 ±0.52	1.34 ±0.47	>0.05	3.38 ±0.42	0.26 ±0.15	<0.001*
<i>OPG</i> gene expression [AU]	0.60 ±0.15	0.66 ±0.19	>0.05	0.14 ±0.02	1.59 ±0.21	<0.001*
<i>RANKL/OPG</i> ratio	2.80 ±0.94	2.20 ±1.02	>0.05	24.70 ±6.80	0.17 ±0.04	<0.001*
Histomorphometry (bone area percentage [%])	39.99 ±4.90	41.07 ±7.70	>0.05	22.70 ±2.10	85.59 ±2.60	<0.001*

Data expressed as mean ± standard deviation ( $M \pm SD$ ) for 4 rats ( $n = 4$ ). BM-MSCs – bone marrow mesenchymal stem cells; BMD – bone mineral density; AU – arbitrary unit (relative expression); \* statistically significant.

## RT-PCR results

At the 1<sup>st</sup> sacrifice time there was no significant difference between the osteoporotic and BM-MSCs groups in terms of gene expression ( $p > 0.05$ ). However, at the 2<sup>nd</sup> sacrifice time there was a significant decrease in *RANKL* and a significant increase in *OPG* gene expression in the BM-MSCs group as compared to the osteoporotic group ( $p < 0.001$ ) (Table 2).

## *RANKL/OPG* ratio in the study groups

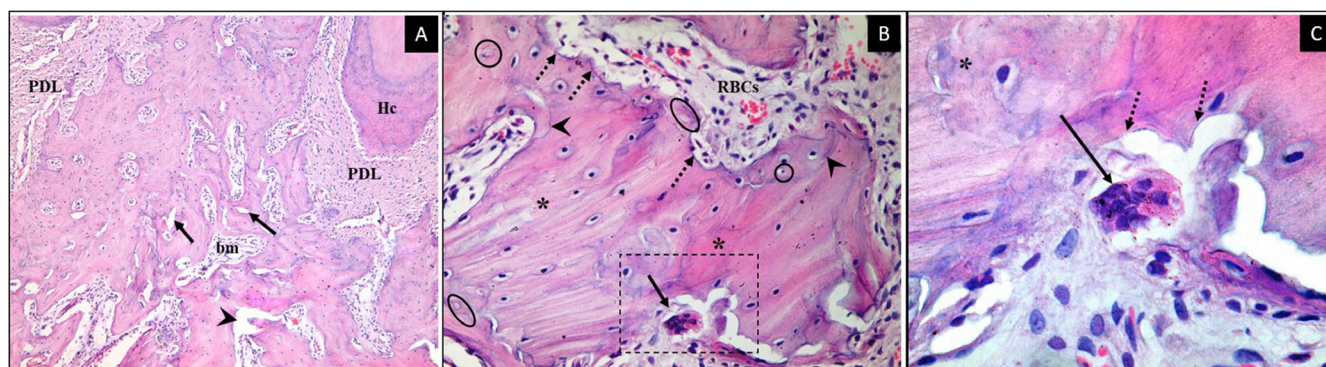
At the 1<sup>st</sup> sacrifice time there was no significant difference between the osteoporotic and BM-MSCs groups in terms of *RANKL/OPG* ratio ( $p > 0.05$ ). However, at the 2<sup>nd</sup> sacrifice time there was a significant decrease in the *RANKL/OPG* ratio in the BM-MSCs group as compared to the osteoporotic group ( $p < 0.001$ ) (Table 2).

## Histopathological results

The histopathological examination of the alveolar bone in the osteoporotic group at the 1<sup>st</sup> sacrifice time showed clear signs of osteoporosis, such as multiple osteoporotic

cavities, scalloped resorptive pits and widened BM cavities surrounded by thin bone trabeculae. Bone marrow cavities showed areas of extravasated red blood cells (RBCs). Cellular degeneration was demonstrated by the diminished osteoblastic lining of BM cavities, the presence of shrunken osteocytes, empty lacunae, and bone areas free of osteocytes. Multinucleated osteoclasts in Howship's lacunae and reversal lines were also observed (Fig. 2).

The histopathological examination of the alveolar bone in the BM-MSCs group at the 1<sup>st</sup> sacrifice time revealed some signs of healing, even though BM cavities were still wide. Bone lamellae showed a more homogenous and better organized architecture. Chronic inflammatory cell infiltration was detected. In addition, congested and dilated blood vessels were present. Some of widened BM cavities regained their osteoblastic lining, although they were still surrounded by thin bone trabeculae. A few osteoporotic and resorptive cavities were still observed. Areas of fatty degeneration were spotted where BM cavities contained multiple adipocytic cells. Regions of newly formed woven bone were noticed with disorganized fibers and osteocytes that were rounder, larger and less regularly spaced than the ones in the lamellar bone. Areas of parallel fibered bone were also found. It appeared as a transitional

**Fig. 2.** Photomicrographs of the osteoporotic group at the 1<sup>st</sup> sacrifice time

A – multiple bone marrow (BM) cavities (bm), some with diminished osteoblastic lining (arrow head), multiple osteoporotic cavities (arrows), hypercementosis (Hc), and the periodontal ligaments (PDL) with degenerated areas (×100 magnification); B – widening and scalloping of BM cavities (dotted arrows) with extravasated red blood cells (RBCs), osteocytes shrunken in their lacunae (circles), empty lacunae (ovals), areas free of osteocytes (asterisks), reversal lines (arrow heads), and a multinucleated osteoclast in a Howship's lacuna (arrow) (×400 magnification); C – higher magnification of the previous figure, showing a multinucleated osteoclast (arrow) in a Howship's lacuna (dotted arrows) (×1,000 magnification).



bone tissue between the newly formed woven bone and the lamellar bone (Fig. 3).

The histopathological examination of the alveolar bone in the osteoporotic group at the 2<sup>nd</sup> sacrifice time presented augmented signs of osteoporosis. Marrow spaces exhibited diminished osteoblastic lining. Wide BM cavities revealed some fatty degeneration with the presence of multiple chronic inflammatory cells. Multiple osteoporotic cavities and malorganized trabecular lamellae were detected. Osteocytes shrunken in their lacunae and some other empty lacunae were observed. Bone resting lines were also noticed (Fig. 4).

The histopathological examination of the alveolar bone in the BM-MSCs group at the 2<sup>nd</sup> sacrifice time displayed a great extent of bone healing. Bone marrow cavities returned to their normal size and regained their osteoblastic lining. Thick

trabecular bone areas containing normal healthy osteocytes of normal size and shape, and resting in their lacunae were noticed. Bone resting lines surrounding marrow spaces were observed. Vascular spaces were noticed near the periodontal ligaments (PDLs). Some vascular spaces turned into secondary osteons surrounded by reversal lines. In addition, scalloped bone reversal lines were noticed, demonstrating the active bone formation and healing process (Fig. 5).

## Histomorphometric results

The comparison of the osteoporotic and BM-MSCs groups revealed that the bone area percentage values were not statistically significantly different at the 1<sup>st</sup> sacrifice time ( $p > 0.05$ ), but were statistically significantly different at the 2<sup>nd</sup> sacrifice time ( $p < 0.001$ ) (Table 2).

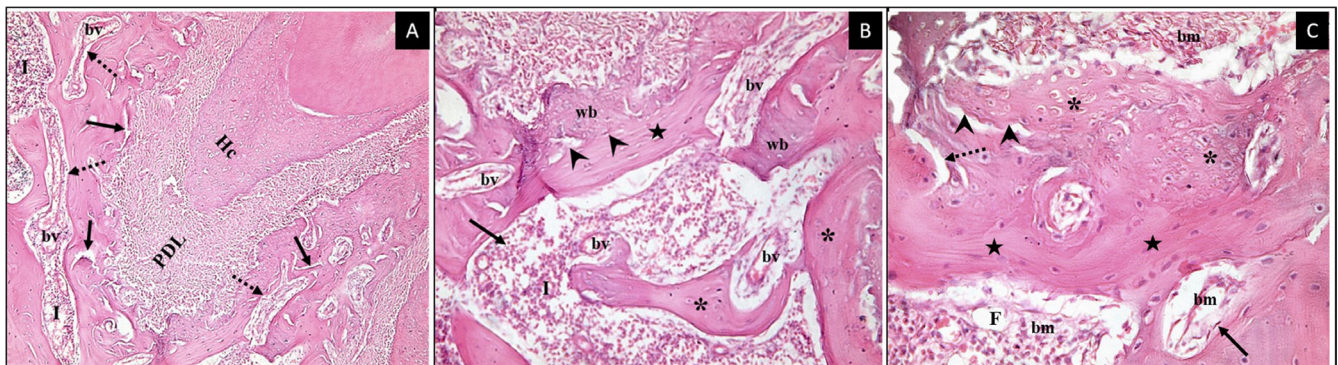


Fig. 3. Photomicrographs of the BM-MSCs group at the 1<sup>st</sup> sacrifice time

A – multiple wide BM cavities (dotted arrows) with some dilated blood vessels (bv) and chronic inflammatory cells (I), some osteoporotic cavities (arrows), hypercementosis (Hc), and a normal periodontal ligament (PDL) (x100 magnification); B – a large BM cavity (arrow) containing dilated blood vessels (bv) and chronic inflammatory cells (I), surrounded by islands of thin bone trabeculae (asterisks), with a line demarcating (arrow heads) areas of newly formed woven bone (wb) and an area of parallel fibered bone (star) (x200 magnification); C – widened BM cavities (bm) with osteoblastic lining (arrow), few areas of fatty degeneration (F) and a resorptive bony cavity (dotted arrow), areas of newly formed woven bone (asterisks) with large osteocytes, demarcated by a scalloped line (arrow heads), and areas of parallel fibered bone (stars) (x400 magnification).

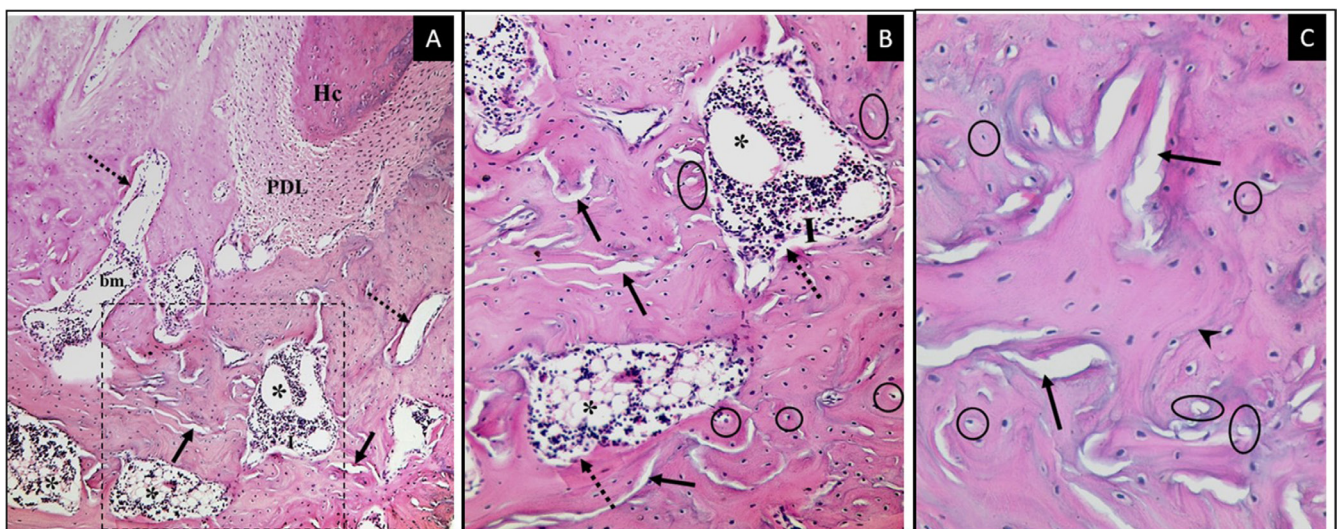


Fig. 4. Photomicrographs of the osteoporotic group at the 2<sup>nd</sup> sacrifice time

A – wide marrow spaces (bm) with diminished osteoblastic lining (dotted arrows), fatty degeneration (asterisks), chronic inflammatory cells (I), osteoporotic cavities (arrows), hypercementosis (Hc), and a normal periodontal ligament (PDL) (x100 magnification); B – higher magnification of the previous figure, showing wide marrow spaces (dotted arrows), fatty degeneration (asterisks), chronic inflammatory cells (I), multiple osteoporotic cavities of varying sizes (arrows), osteocytes shrunken in their lacunae (circles), and empty lacunae (ovals) (x200 magnification); C – multiple wide osteoporotic cavities (arrows), shrunken osteocytes (circles), empty lacunae (ovals), and a bone resting line (arrow head) (x400 magnification).



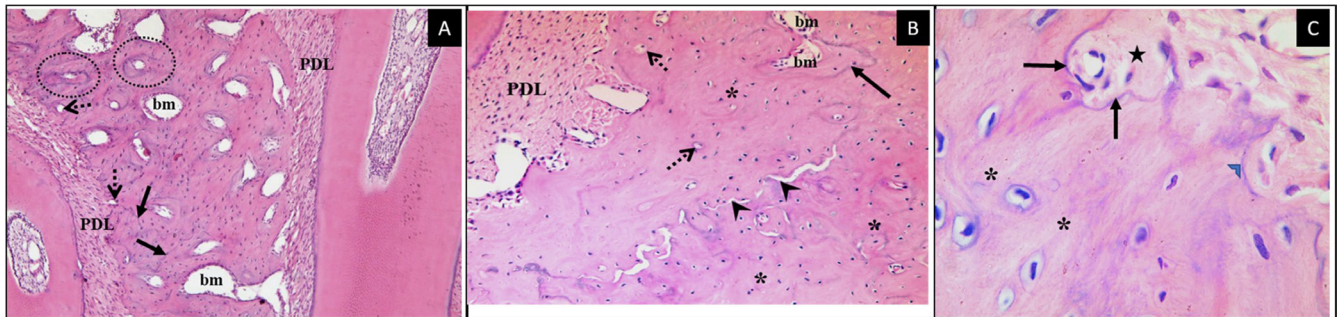


Fig. 5. Photomicrographs of the BM-MSCs group at the 2<sup>nd</sup> sacrifice time

A – alveolar marrow spaces with a complete osteoblastic lining (bm), resting lines (arrows), vascular spaces (dotted arrows), secondary osteons (dotted circles), and normal periodontal ligaments (PDL) (x100 magnification); B – BM cavities with an osteoblastic lining (bm), osteocytes of normal size and shape (asterisks), vascular channels (dotted arrows), a resting line (arrow), reversal lines (arrow heads), and a normal periodontal ligament (PDL) (x200 magnification); C – normal osteocytes in their lacunae (asterisks) and bone reversal lines (arrows) denoting newly formed bone matrix (star) (x1,000 magnification).

## Discussion

The seriousness of osteoporosis lies in it being a totally asymptomatic illness that often remains undiagnosed until it is manifested as a fracture.<sup>2</sup> All of the available kinds of pharmacological treatment are accompanied by multiple side effects, which is why a need for safer treatment options has emerged.<sup>20</sup> Hence, this study aimed to assess the bone healing potential of BM-MSCs in glucocorticoid-induced jawbone osteoporosis.

In the current work, osteoporosis was examined in the mandibular jawbones of adult rats. This is in accordance with Jonasson and Rythén, who stated that the rate of bone turnover in the mandibular alveolar processes might be the fastest in the body; therefore, the initial signs of osteoporosis could be revealed there the earliest.<sup>21</sup>

During the study period, BMD significantly deteriorated in the osteoporotic group. This finding is consistent with Cao et al., who reported that BMD significantly decreased in osteoporotic rats.<sup>22</sup>

At the 2<sup>nd</sup> sacrifice time, *RANKL* gene expression was significantly elevated in the osteoporotic group. This is in agreement with Eghbali-Fatourehchi et al., who proved a significant upregulation of *RANKL* in osteoporotic postmenopausal women.<sup>23</sup> On the other hand, *OPG* gene expression was significantly decreased. This is in accordance with a clinical study in which the delayed phase of osteoporosis caused *OPG* levels to decrease.<sup>24</sup>

In the current investigation, the histopathological changes in the osteoporotic group became more noticeable at the 2<sup>nd</sup> sacrifice time. These observations resemble the findings of previous authors, who observed marked histopathological alterations in the mandibular alveolar bone spongiosa of osteoporotic rats.<sup>17,25</sup> Moreover, the great increase in BM fat content observed at the 2<sup>nd</sup> sacrifice time was demonstrated by former studies, which reported that an increase in circulating glucocorticoids caused fatty tissue infiltration and the expansion of BM adipose tissue.<sup>26,27</sup>

In this study, the histomorphometric analysis confirmed the histopathological architectural changes

in the osteoporotic group. This coincides with the findings of Abuhashish et al., who determined that the morphometric parameters of femur bones were significantly decreased in osteoporotic rats.<sup>28</sup>

In the present work, after injecting the osteoporotic rats with BM-MSCs, BMD significantly increased along the 2 sacrifice periods. This is quite similar to the observations of Hsiao et al., who confirmed that BM-MSCs migrated to bone after an intravenous injection, leading to an increased BMD and restored bone volume in an ovariectomized mouse model.<sup>29</sup> This might be attributed to the ability of the transplanted MSCs to migrate to the site of injury and produce immunomodulatory cytokines and growth factors, helping local cells to recover and inducing the recruitment of new cells in the area.<sup>8</sup>

In the BM-MSCs group, *RANKL* gene expression significantly decreased at the 2<sup>nd</sup> sacrifice time as compared to the osteoporotic group. These results are supported by Li et al., who found BM-MSCs to alleviate the symptoms of arthritis mainly by decreasing the levels of *RANKL* gene expression.<sup>30</sup> On the other hand, the level of *OPG* gene expression showed a significant increase. This coincides with the results of Oshita et al., who reported that human MSCs produced *OPG* continuously, at both the mRNA and protein levels, which inhibited the osteoclastogenesis process.<sup>31</sup>

In the current work, the histopathological findings in the BM-MSCs group revealed gradual improvement between the 1<sup>st</sup> and 2<sup>nd</sup> sacrifice times. This is in agreement with Freitas et al., who demonstrated that the newly formed bone was observed 4 weeks after the injection of BM-MSCs in rat calvarial defects.<sup>32</sup> This is also supported by Kim et al., who proved that MSCs reduced the progression of senile osteoporosis by sustaining osteocalcin levels in the circulation, which resulted in improved bone microarchitecture.<sup>33</sup>

Concerning the histomorphometric analysis, the BM-MSCs group showed a significant progressive increase in bone volume at the 2<sup>nd</sup> sacrifice time. This is in agreement with de Melo Ocarino et al., who found that the greatest bone volume was achieved 2 months after injecting the osteoporotic rats with differentiated BM-MSCs.<sup>34</sup>

The osteoporosis model should be further studied on animals with bone morphology closer to humans, as osteogenic healing in rats far exceeds that of a human. Also, more research techniques are needed to fully understand the healing mechanism of BM-MSCs in the treatment of osteoporosis. Furthermore, more clinical trials should be conducted to determine the proper effective human dosage of BM-MSCs in treating osteoporosis.

## Conclusions

After assessing all the DEXA, RT-PCR, histopathological, and histomorphometric results, it was confirmed that BM-MSCs had a positive effect on bone healing potential. It was also shown that the healing progress was achieved gradually along the experiment duration. Therefore, it can be concluded that BM-MSCs could act as an effective treatment option for osteoporosis. However, further experiments with larger sample sizes are recommended to confirm these results.

## Ethics approval and consent to participate

This experiment was conducted at the animal house at the Faculty of Medicine of Cairo University, Egypt, after obtaining the approval of the Institutional Animal Care and Use Committee (IACUC) (CU-III-F-73-17).

## Data availability

All data generated and/or analyzed during this study is included in this published article.


## Consent for publication


Not applicable.


## ORCID iDs

Tasneem Soliman  <https://orcid.org/0000-0003-0908-2113>

Zoba Ali  <https://orcid.org/0000-0003-1713-8586>

Mohamed Zayed  <https://orcid.org/0000-0001-8453-6088>

Dina Sabry  <https://orcid.org/0000-0002-6720-3385>

Nermeen AbuBakr  <https://orcid.org/0000-0003-2962-0070>

## References

- Kanis JA, Melton LJ 3<sup>rd</sup>, Christiansen C, Johnston CC, Khaltaev N. The diagnosis of osteoporosis. *J Bone Miner Res*. 1994;9(8):1137–1141. doi:10.1002/jbmr.5650090802
- Compston J, Cooper A, Cooper C, et al. UK clinical guideline for the prevention and treatment of osteoporosis. *Arch Osteoporos*. 2017;12(1):43. doi:10.1007/s11657-017-0324-5
- Anil S, Preethanath RS, AlMoharib HS, Kamath KP, Anand PS. Impact of osteoporosis and its treatment on oral health. *Am J Med Sci*. 2013;346(5):396–401. doi:10.1097/MAJ.0b013e31828983da
- Swanson C, Lorentzon M, Conaway HH, Lerner UH. Glucocorticoid regulation of osteoclast differentiation and expression of receptor activator of nuclear factor-kappaB (NF-kappaB) ligand, osteoprotegerin, and receptor activator of NF-kappaB in mouse calvarial bones. *Endocrinology*. 2006;147(7):3613–3622. doi:10.1210/en.2005-0717
- Reid IR. Efficacy, effectiveness and side effects of medications used to prevent fractures. *J Intern Med*. 2015;277(6):690–706. doi:10.1111/joim.12339
- Tu KN, Lie JD, Wan CKV, et al. Osteoporosis: A review of treatment options. *PT*. 2018;43(2):92–104. PMID:29386866. PMCID:PMC5768298.
- Rubin KH, Möller S, Choudhury A, et al. Cardiovascular and skeletal safety of zoledronic acid in osteoporosis observational, matched cohort study using Danish and Swedish health registries. *Bone*. 2020;134:115296. doi:10.1016/j.bone.2020.115296
- Wang C, Meng H, Wang X, Zhao C, Peng J, Wang Y. Differentiation of bone marrow mesenchymal stem cells in osteoblasts and adipocytes and its role in treatment of osteoporosis. *Med Sci Monit*. 2016;22:226–233. doi:10.12659/msm.897044
- Macías I, Alcorta-Sevillano N, Rodríguez CI, Infante A. Osteoporosis and the potential of cell-based therapeutic strategies. *Int J Mol Sci*. 2020;21(5):1653. doi:10.3390/ijms21051653
- Liu HY, Wu ATH, Tsai CY, et al. The balance between adipogenesis and osteogenesis in bone regeneration by platelet-rich plasma for age-related osteoporosis. *Biomaterials*. 2011;32(28):6773–6780. doi:10.1016/j.biomaterials.2011.05.080
- Bronckers AL, Sasaguri K, Engelse MA. Transcription and immunolocalization of Runx2/Cbfa1/PeBP2alphaA in developing rodent and human craniofacial tissues: Further evidence suggesting osteoclasts phagocytose osteocytes. *Microsc Res Tech*. 2003;61(6):540–548. doi:10.1002/jemt.10377
- Jiang Y, Zhang P, Zhang X, Lv L, Zhou Y. Advances in mesenchymal stem cell transplantation for the treatment of osteoporosis. *Cell Prolif*. 2021;54(1):e12956. doi:10.1111/cpr.12956
- AbuBakr N, Haggag T, Sabry D, Salem ZA. Functional and histological evaluation of bone marrow stem cell-derived exosomes therapy on the submandibular salivary gland of diabetic Albino rats through TGFβ/Smad3 signaling pathway. *Heliyon*. 2020;6(4):e03789. doi:10.1016/j.heliyon.2020.e03789
- Dominici M, Le Blanc K, Mueller I, et al. Minimal criteria for defining multipotent mesenchymal stromal cells. The International Society for Cellular Therapy position statement. *Cytotherapy*. 2006;8(4):315–317. doi:10.1080/14653240600855905
- Uejima S, Okada K, Kagami H, Taguchi A, Ueda M. Bone marrow stromal cell therapy improves femoral bone mineral density and mechanical strength in ovariectomized rats. *Cytotherapy*. 2008;10(5):479–489. doi:10.1080/14653240802071616
- Chutkerashvili G, Menabde G, Chutkerashvili K, Dotiashvili D, Amirashvili I. The treatment of osteoporosis through transplantation of bone marrow stem cells in the experiments performed on rats. *Georgian Med News*. 2012;3(204):88–92. PMID:22573756.
- Ezzat BA, Abbass MM. The ability of H1 or H2 receptor antagonists or their combination in counteracting the glucocorticoid-induced alveolar bone loss in rats. *J Oral Pathol Med*. 2014;43(2):148–156. doi:10.1111/jop.12104
- Leary S, Underwood W, Anthony R, et al.; the Panel of Euthanasia. *AVMA Guidelines for the Euthanasia of Animals: 2013 Edition*. Schaumburg, IL: American Veterinary Medical Association; 2013.
- Gao SG, Li KH, Xu M, et al. Bone turnover in passive smoking female rat: Relationships to change in bone mineral density. *BMC Musculoskelet Disord*. 2011;12:131. doi:10.1186/1471-2474-12-131
- Lin H, Sohn J, Shen H, Langhans MT, Tuan RS. Bone marrow mesenchymal stem cells: Aging and tissue engineering applications to enhance bone healing. *Biomaterials*. 2019;203:96–110. doi:10.1016/j.biomaterials.2018.06.026
- Jonasson G, Rythén M. Alveolar bone loss in osteoporosis: A loaded and cellular affair? *Clin Cosmet Invest Dent*. 2016;8:95–103. doi:10.2147/CCIDE.S92774
- Cao H, Zhang Y, Qian W, et al. Effect of icariin on fracture healing in an ovariectomized rat model of osteoporosis. *Exp Ther Med*. 2017;13(5):2399–2404. doi:10.3892/etm.2017.4233
- Eghbali-Fatourehchi G, Khosla S, Sanyal A, Boyle WJ, Lacey DL, Riggs BL. Role of RANK ligand in mediating increased bone resorption in early postmenopausal women. *J Clin Invest*. 2003;111(8):1221–1230. doi:10.1172/JCI17215
- Gurban C, Zosin I, Sfrijan F, et al. The OPG/sRANKL system and the low bone mineral density in postmenopausal osteoporosis. *Acta Endo (Buc)*. 2009;5(1):27–40. doi:10.4183/aeb.2009.27



25. Abu Taleb OM, Wissa MY, Abou El Nour RK, Awad HA, Moussa NM. Potential effectiveness of exenatide in experimentally-induced osteoporosis. *Egypt Rheumatol.* 2020;42(1):57–62. doi:10.1016/j.ejr.2019.06.003
26. Cawthorn WP, Scheller EL, Parlee SD, et al. Expansion of bone marrow adipose tissue during caloric restriction is associated with increased circulating glucocorticoids and not with hypoleptinemia. *Endocrinology.* 2016;157(2):508–521. doi:10.1210/en.2015-1477
27. Sherif H, El Masry NA, Kawana KY, Khalil NM. Effect of bisphosphonates on the alveolar bone of rats with glucocorticoids induced osteoporosis. *Alexandria Dent J.* 2019;44(3):65–70. doi:10.21608/ADJALEXU.2019.63560
28. Abuohashish HM, Ahmed MM, Al-Rejaie SS, Eltahir KE. The anti-depressant bupropion exerts alleviating properties in an ovariectomized osteoporotic rat model. *Acta Pharmacol Sin.* 2015;36(2):209–220. doi:10.1038/aps.2014.111
29. Hsiao FSH, Cheng CC, Peng SY, et al. Isolation of therapeutically functional mouse bone marrow mesenchymal stem cells within 3 h by an effective single-step plastic-adherent method. *Cell Prolif.* 2010;43(3):235–248. doi:10.1111/j.1365-2184.2010.00674.x
30. Li F, Li X, Liu G, Gao C, Li X. Bone marrow mesenchymal stem cells decrease the expression of RANKL in collagen-induced arthritis rats via reducing the levels of IL-22. *J Immunol Res.* 2019;2019:8459281. doi:10.1155/2019/8459281
31. Oshita K, Yamaoka K, Udagawa N, et al. Human mesenchymal stem cells inhibit osteoclastogenesis through osteoprotegerin production. *Arthritis Rheum.* 2011;63(6):1658–1667. doi:10.1002/art.30309
32. Freitas GP, Lopes HB, Souza AT, et al. Cell therapy: Effect of locally injected mesenchymal stromal cells derived from bone marrow or adipose tissue on bone regeneration of rat calvarial defects. *Sci Rep.* 2019;9(1):13476. doi:10.1038/s41598-019-50067-6
33. Kim YH, Park M, Cho KA, et al. Tonsil-derived mesenchymal stem cells promote bone mineralization and reduce marrow and visceral adiposity in a mouse model of senile osteoporosis. *Stem Cells Dev.* 2016;25(15):1161–1171. doi:10.1089/scd.2016.0063
34. de Melo Ocarino N, Boeloni JN, Jorgetti V, Gomes DA, Goes AM, Serakides R. Intra-bone marrow injection of mesenchymal stem cells improves the femur bone mass of osteoporotic female rats. *Connect Tissue Res.* 2010;51(6):426–433. doi:10.3109/03008201003597049